Combining Mechanical Ball-milling with Melt-polymerization to Fabricate Polyimide Covalent Organic Frameworks towards High-Performance Sodium-Ion Batteries

Yu Wu[a], Xu Han[b], Hailong Hu[a], Hongyin Hu[a], Jinyan Wang[a], Yaoyao Deng[c], Fang Duan[a], Hongwei Gu[b], Mingliang Du[a], Shuanglong Lu[a]*

[a]Key Laboratory of Synthetic and Biological Colloids, Ministry of Education, School of Chemical and Material Engineering, Jiangnan University, Wuxi, Jiangsu 214122, P. R. China. E-mail: lushuanglong@jiangnan.edu.cn

[b]Key Laboratory of Organic Synthesis of Jiangsu Province, College of Chemistry, Chemical Engineering and Materials Science, Collaborative Innovation Center of Suzhou Nano Science and Technology, Soochow University, Suzhou 215123, China.

[c]School of Chemical Engineering and Materials Science, Changzhou Institute of Technology, Changzhou 213032, China.

Materials

1,3,5-tris-(4-aminophenyl) triazine (TAPT), 4,4,4 -(1,3,5-triazine-2,4,6-triyl) tris (([1,1 -biphenyl]-4-amine)) (TTBT) was obtained from the Jilin Chinese Academy of Sciences-Yanshen Technology Co., Ltd. pyromellitic acid (PMA) and Benzoic anhydride were purchased from Aladdin. N-methyl pyrrolidone (NMP), Methanol and DMF were obtained from Shanghai Titan Scientific Co., Ltd. Other solvents, reagents, and chemicals were utilized without any further purification.

Characterizations

Powder X-ray diffraction (PXRD) analysis was conducted using a Bruker D8 Advance diffractometer equipped with Cu Kα radiation. The Fourier transform infrared (FT-IR) spectra of the synthetic materials structures were obtained with a Nicolet iS50 spectrometer. Solid-state ^{13}C cross-polarization magic-angle spinning (CP-MAS) NMR spectra were recorded on a Bruker 400 MHz spectrometer. The Brunauer–Emmett–Teller (BET) specific surface area was measured via N_2 adsorption at 77 K using an ASAP 2460 surface area analyzer. The morphology of the samples was investigated using scanning electron microscopy (SEM, S-4800) and transmission electron microscopy (TEM, JEM-2100plus). X-ray photoelectron spectroscopy (XPS) measurements were performed with a Thermo Scientific K-Alpha spectrometer.

Synthesis of $COF_{PMA\text{-}TAPT}$ and $COF_{PMA\text{-}TTBT}$

PMA 76.2 mg (0.3 mmol), TAPT 70.8 mg (0.2 mmol) or TTBT 116.6 mg (0.2 mmol) and benzoic acid 146.6 mg (1.2 mmol) were weighed and thoroughly ground in a mortar for 15 minutes to ensure that they were well mixed. The resulting mixture was transferred to a test tube and degassed by three nitrogen purges. The tubes were then flame sealed under vacuum. The sealed tubes were then heated in an oven at 200 °C for 120 h. After cooling to room temperature, the product was washed three times sequentially with DMF and methanol. The resulting powder was Soxhlet extracted with methanol for 24 hours. Finally, the powder was collected and dried under vacuum at 60 °C

Electrochemical Measurements

The active materials ($COF_{PMA\text{-}TAPT}$ and $COF_{PMA\text{-}TTBT}$, 70 wt.%), conductive additive (Super P, 20 wt.), and PVDF (10 wt.%) were mixed to prepare a slurry using PVDF/NMP (20

g/L). The slurry was sealed and stirred for 12 hours, then coated onto a copper foil substrate and dried in a vacuum oven at 80°C for 12 hours. The copper foil with the coated active material was then cut into 14 mm diameter disks to serve as working electrodes, with an active material loading of 0.6–0.8 mg·cm^{-2}. Sodium foil was used as the counter electrode, and the electrolyte was 1.0 M $NaPF_6$ dissolved in a DEG: DME (1:1 v/v) solution. CR2032 coin cells were assembled using a microfiber glass membrane (Whatman GF/D, Aldrich) as the separator, and the assembly was conducted in an argon-filled glove box (H_2O, O_2 < 0.01 ppm). Battery performance was evaluated using a Land CT 2001 A instrument for constant current charge-discharge tests within a voltage range of 0.01–3.0 V (vs. Na+/Na) at various current densities. Cyclic voltammetry (CV) was performed in a voltage range of 0.01–3.0 V (vs. Na+/Na) using a CHI 660 electrochemical workstation, and electrochemical impedance spectroscopy (EIS) was conducted on a Gamry Interface 5000 with a frequency range from 100,000 Hz to 0.01 Hz and an AC oscillation amplitude of 10 mV.

By correlating the voltage sweep rate with the resulting peak current response, it is possible to distinguish between diffusive and pseudocapacitive behavior of the cell. The presence of pseudo-capacitance is assessed by calculating the b-value.

$$i = av^b \quad e\text{quation 1}$$

In addition, the pseudo-capacitance contribution at a specific scan rate can be calculated by measuring the current response at different potentials. This contribution is obtained by dividing the area under the fitted curve by the total area of the cyclic voltammetry (CV) curve. In this context, k_1 and k_2 are adjustable constants, V represents the voltage, and v denotes the scan rate. Specifically, k_1v reflects the current contribution attributed to capacitive behavior, while $k_2v^{1/2}$ accounts for the current contribution governed by diffusion processes.

$$i(V) = k_1v + k^{1/2}_2 \quad e\text{quation 2}$$

Theoretical capacity.

The theoretical capacity C_t (mAh g^{-1}) was calculated using the equation:

$$C_t = nF/(3.6Mw) \quad \text{Equation 3}$$

where n represents the number of charge carriers (for the repeat units of $COF_{PMA\text{-}TAPT}$ and $COF_{PMA\text{-}TTBT}$, n=2), F is the Faraday constant (96484 C mol^{-1}), and M_w denotes the equivalent molecular weight of the active materials. The equivalent molecular weight is defined as the molecular weight of the unit cell of the COFs or control compound divided by the number of electrons involved in the charge transfer process. In the $COF_{PMA\text{-}TAPT}$ and $COF_{PMA\text{-}TTBT}$ systems, the molecular weight of the repeat imide units (M_A) is 214. The molecular weights of the repeating units for TAPT (M_B) and TTBT (M_C) are 306 and 537, respectively (Scheme S1). Among others each triazine unit contributes three electrons and the imine unit contributes two electrons, so a repeating unit provides two electrons. Based on this electron contribution, the theoretical capacities of $COF_{PMA\text{-}TAPT}$ and $COF_{PMA\text{-}TTBT}$ were calculated to be 256 mAh g^{-1} and 187 mAh g^{-1}, respectively.

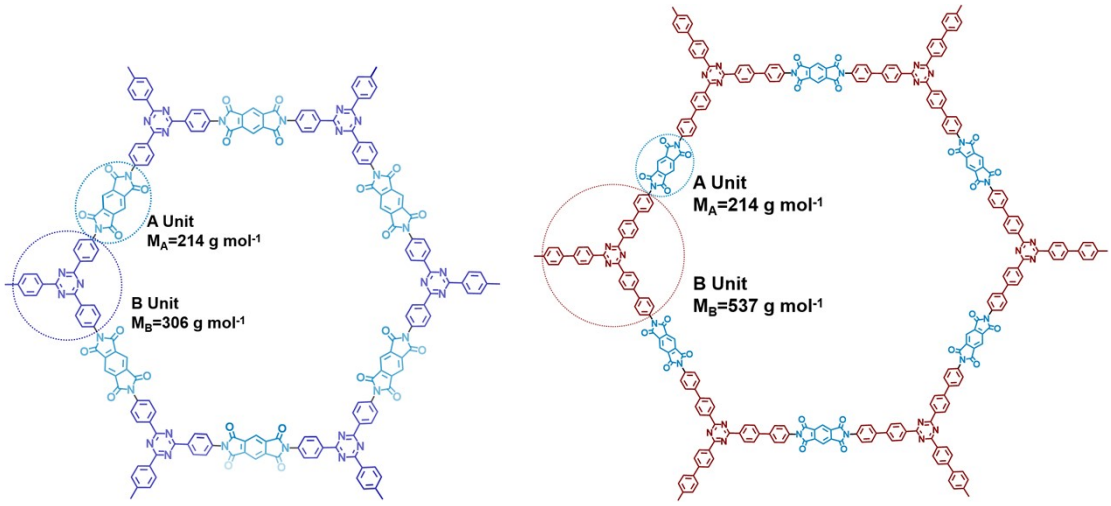

Scheme S1: Chemical structure of $COF_{PMA\text{-}TAPT}$ and $COF_{PMA\text{-}TTBT}$.

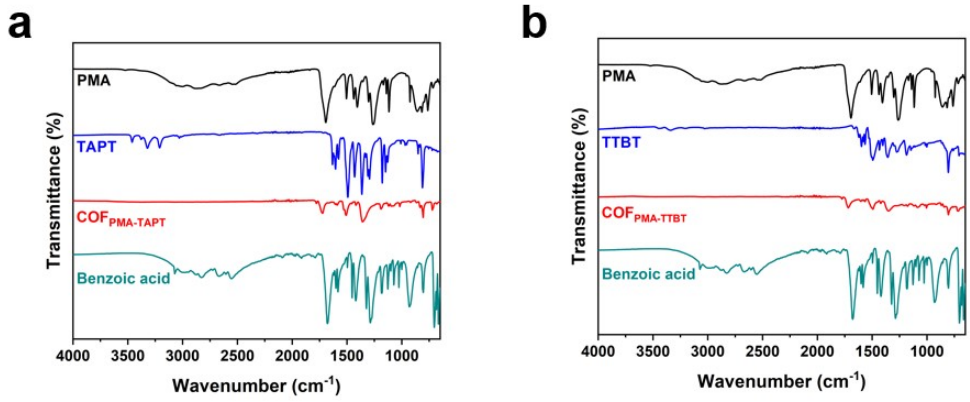

Fig. S1. FT-IR spectra of $COF_{PMA-TAPT}$ (a) and $COF_{PMA-TTBT}$ (b), respectively.

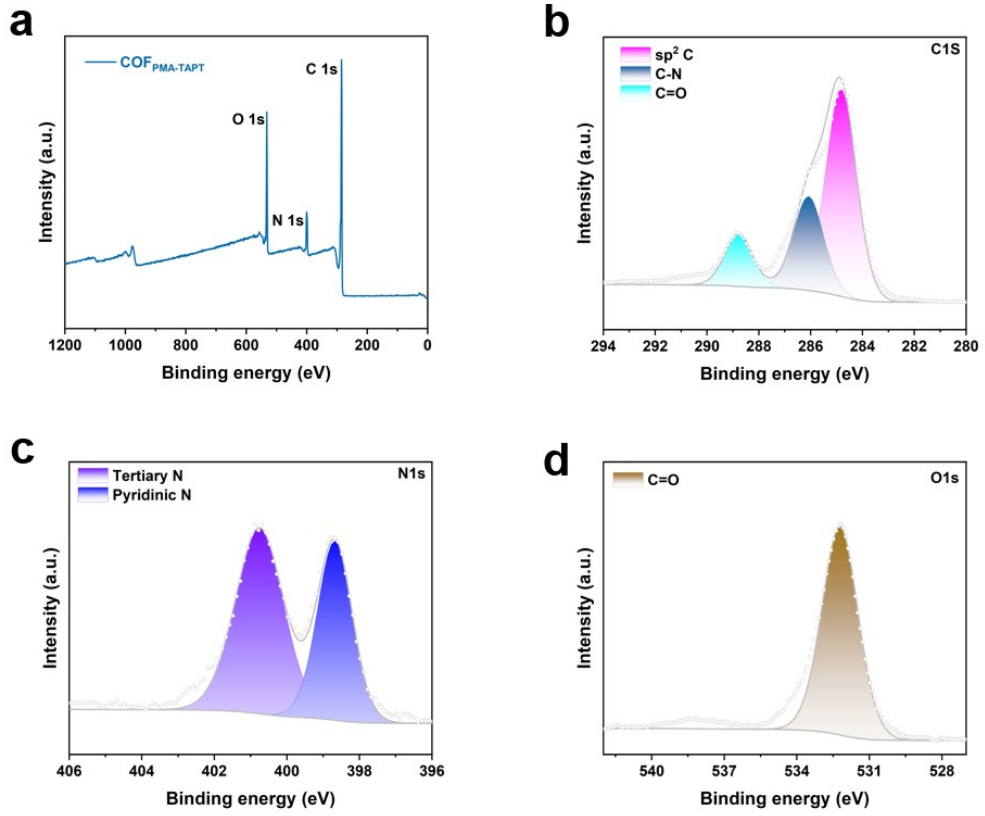

Fig. S2. XPS survey for $COF_{PMA-TAPT}$ (a); C 1s (b), N 1s (c) and O 1s (d) XPS spectra of $COF_{PMA-TAPT}$.

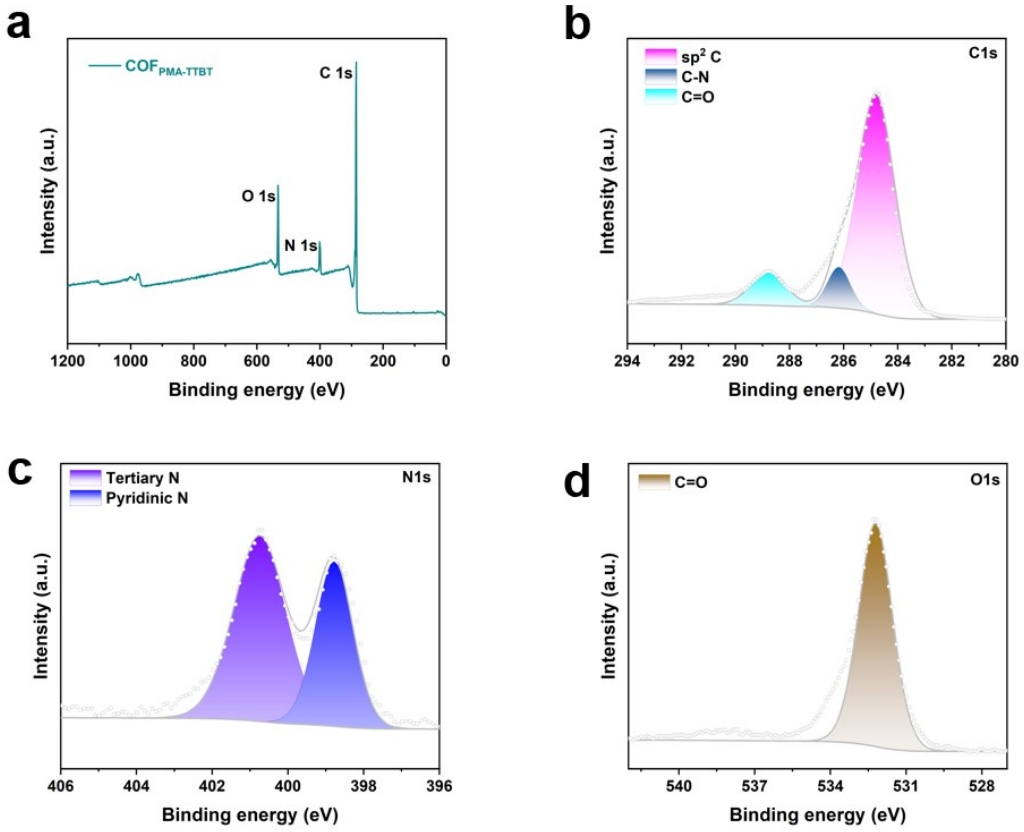

Fig. S3. XPS survey for $COF_{PMA\text{-}TTBT}$ (a); C 1s (b), N 1s (c) and O 1s (d) XPS spectra of $COF_{PMA\text{-}TTBT}$.

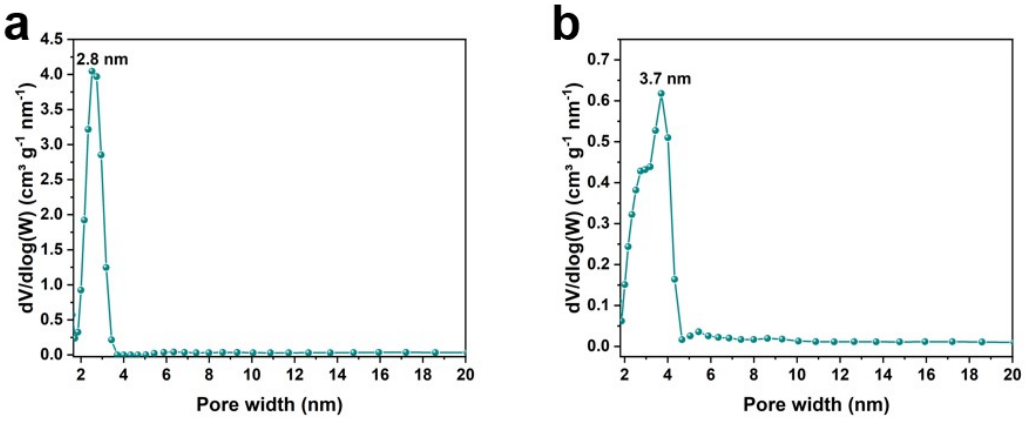

Fig. S4. The pore size distribution of $COF_{PMA\text{-}TAPT}$ (a) and $COF_{PMA\text{-}TTBT}$ (b).

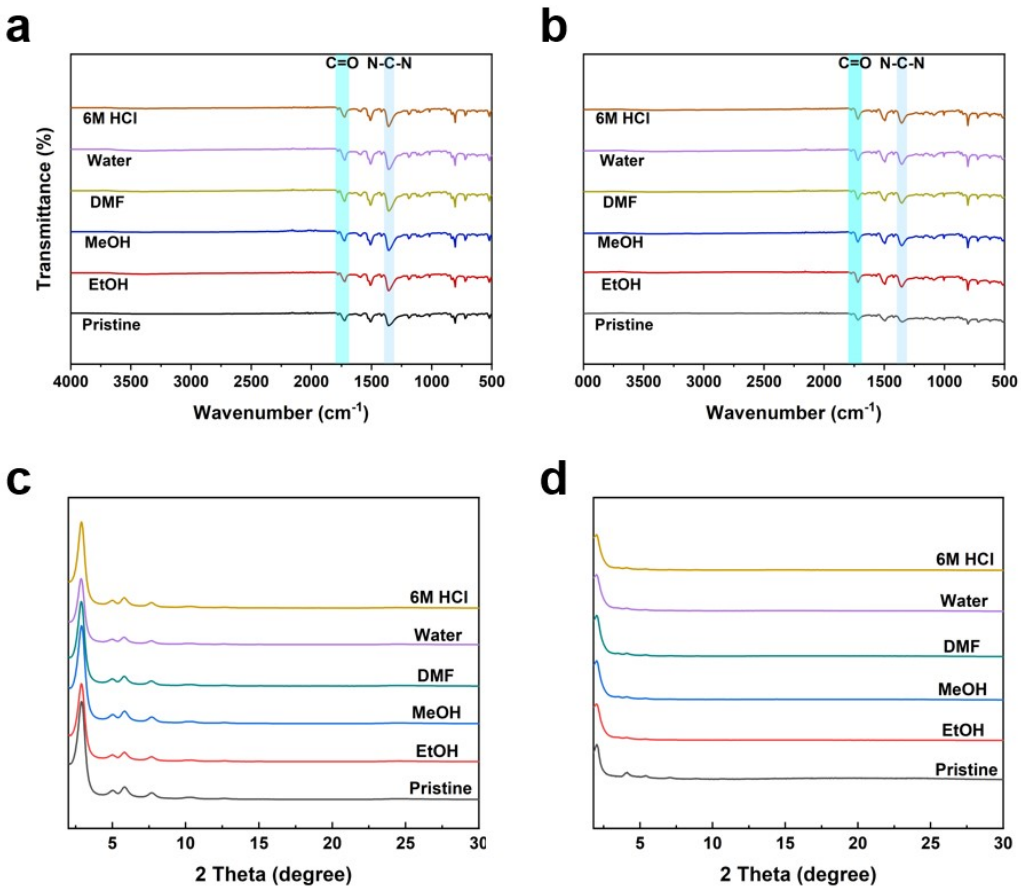

Fig. S5. FT-IR spectra and PXRD of $COF_{PMA\text{-}TAPT}$ (a, c) and $COF_{PMA\text{-}TTBT}$ (b, d) after exposure to 6M HCl, Water, DMF, MeOH and EtOH for 48 hours.

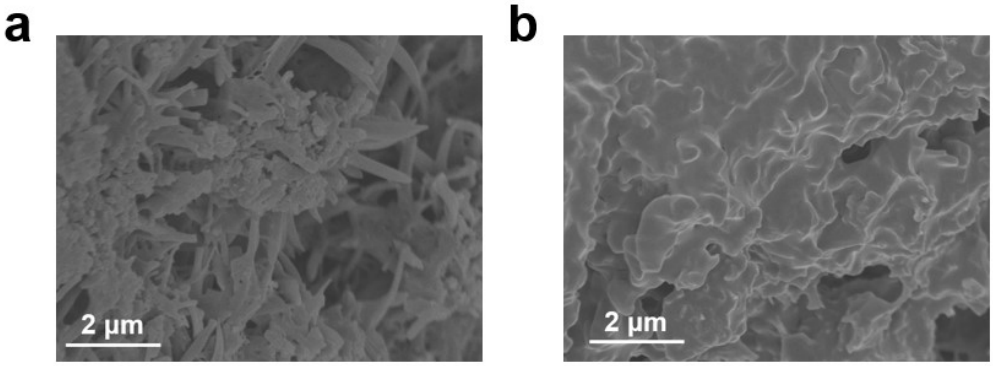

Fig. S6. SEM images of $COF_{PMA\text{-}TAPT}$ (a) and $COF_{PMA\text{-}TTBT}$ (b).

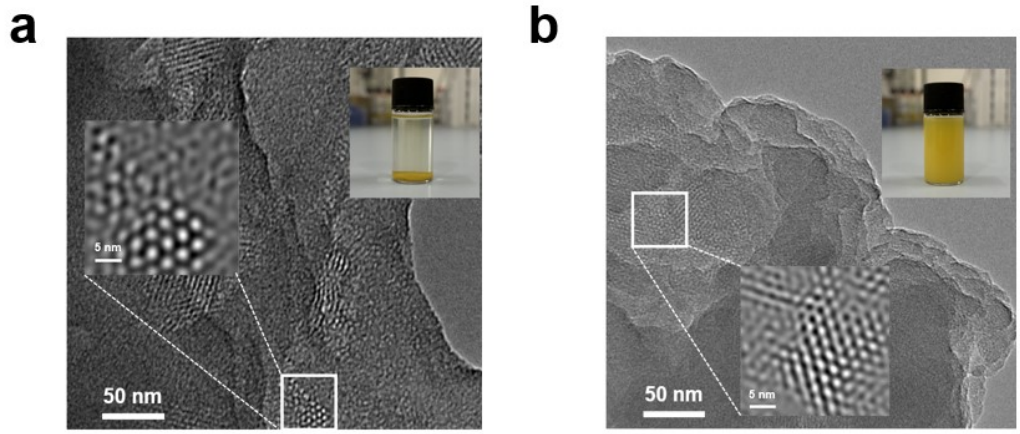

Fig. S7. TEM image, HR-TEM image of $COF_{PMA\text{-}TTBT}$ (a) and after stripping $COF_{PMA\text{-}TTBT}$ (b).

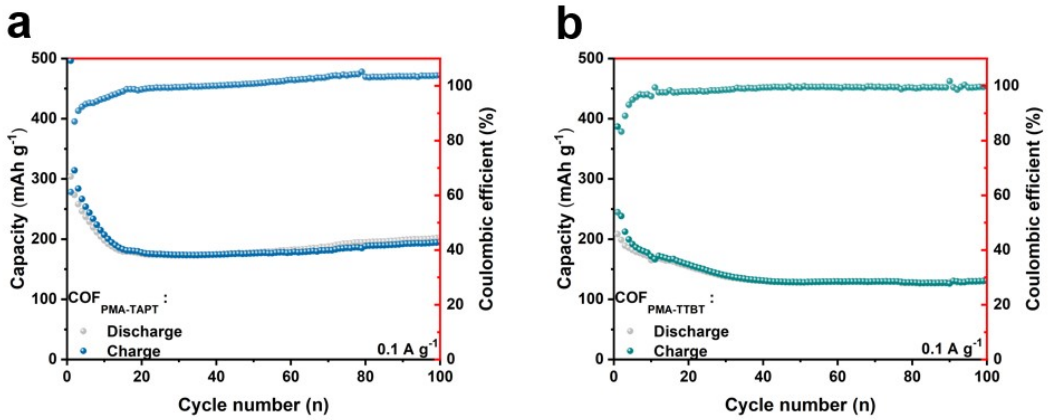

Fig. S8. Cycling stability and Coulombic efficiency of $COF_{PMA\text{-}TAPT}$ (a) and $COF_{PMA\text{-}TTBT}$ (b) at 0.1 A g^{-1}.

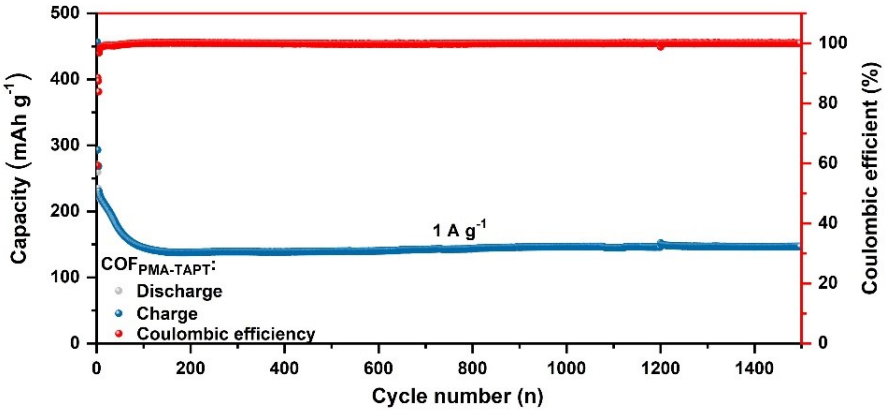

Fig. S9. Cycling stability and Coulombic efficiency of $COF_{PMA\text{-}TAPT}$ at 1 A g^{-1}.

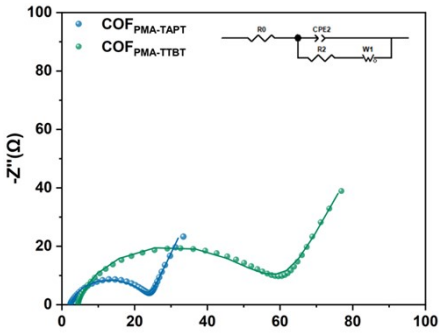

Fig. S10. Electrochemical Impedance Characteristics (EIS) of $COF_{PMA\text{-}TAPT}$ and $COF_{PMA\text{-}TTBT}$.

Table S1. Fitted values in the equivalent circuit for EIS data of $COF_{PMA\text{-}TAPT}$ and $COF_{PMA\text{-}TTBT}$.

	R2 (Ω)	R0 (Ω)	CPE2 (F)	W1 (Ω)
$COF_{PMA\text{-}TAPT}$	19.11	2.46	3.09×10^{-6}	7.16
$COF_{PMA\text{-}TTBT}$	45.61	4.31	1.41×10^{-6}	34.18

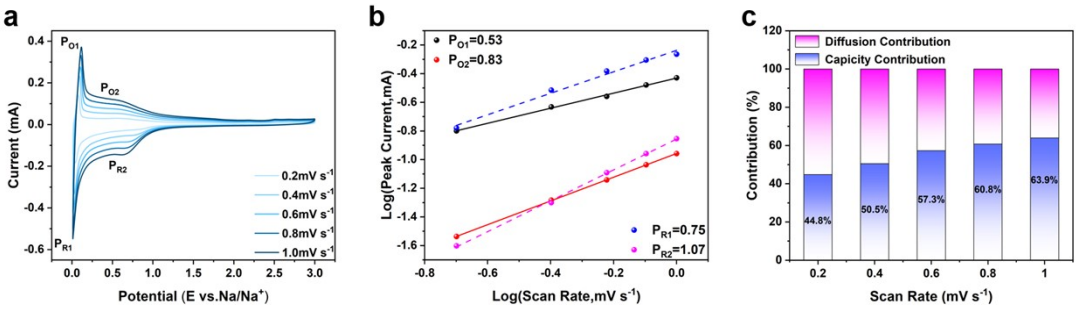

Fig. S11. CV patterns of $COF_{PMA\text{-}TAPT}$ at different scan rates (a); Plots of log current versus log scan rate for $COF_{PMA\text{-}TAPT}$ (b); Capacitive contribution and Diffusion contribution currents at different scan rates for $COF_{PMA\text{-}TAPT}$ (c).

Table S2. Performance of $COF_{PMA-TAPT}$, $COF_{PMA-TTBT}$ and some typical COFs prepared in other methods as anodes for sodium-ion batteries.

Active Material	**Synthesis method**	**Specific capacity/ Current density**	**Active site utilization (0.1 A g^{-1})**	**Ref**
$COF_{PMA-TAPT}$	**melt-polymerization and ball-milling**	**253.4 mAh g^{-1} @0.1 A g^{-1} 176.3 mAh g-1@1 A g^{-1}**	**83.5%**	**This work**
$COF_{PMA-TTBT}$	**melt-polymerization and ball-milling**	**157.7 mAh g^{-1} @0.1 A g^{-1} 124 mAh g-1@1 A g^{-1}**	**84.3%**	**This work**
TFPB-TAPT COF	solvothermal method	170 mAh g^{-1} @0.1 A g^{-1} 145 mAh g-1@0.2 A g^{-1}	72.9%	J. Mater. Chem. A, 2018, 6, 16655
S@TAPT-COFs	solvothermal method	109.3 mAh g^{-1}@0.1 A g^{-1} 73.2 mAh g^{-1}@1 A g^{-1}	NA	Chem. Eng. J., 453, 2023, 139607
TPDA-NDI-50%CNT	solvothermal method	120 mAh g^{-1}@0.05 A g^{-1} 88 mAh g^{-1}@1 A g^{-1}	70% (0.05 A g^{-1})	Small, 2024, 2407525
TAPB-NDA@CNT50	microwave-assisted method	101.4 mAh g^{-1}@0.1 A g^{-1} 71.5 mAh g^{-1}@1 A g^{-1}	73.2%	Small, 2024, 2406173